Modeling large-scale inundation of Amazonian seasonally flooded wetlands

Matthew Wilson,[1] Paul Bates,[2] Doug Alsdorf,[3] Bruce Forsberg,[4] Matthew Horritt,[5] John Melack,[6] Frédéric Frappart,[7] and James Famiglietti[7]

[1]   This paper presents the first application and validation of a 2D hydrodynamic model of the Amazon at a large spatial scale. The simulation results suggest that a significantly higher proportion of total flow is routed through the floodplain than previously thought. We use the hydrodynamic model LISFLOOD-FP with topographic data from the Shuttle Radar Topography Mission to predict floodplain inundation for a 240 × 125 km section of the central Amazon floodplain in Brazil and compare our results to satellite-derived estimates of inundation extent, existing gauged data and satellite altimetry. We find that model accuracy is good at high water (72% spatial fit; 0.99 m root mean square error in water stage heights), while accuracy drops at low water (23%; 3.17 m) due to incomplete drainage of the floodplain resulting from errors in topographic data and omission of floodplain hydrologic processes from this initial model. **Citation:** Wilson, M., P. Bates, D. Alsdorf, B. Forsberg, M. Horritt, J. Melack, F. Frappart, and J. Famiglietti (2007), Modeling large-scale inundation of Amazonian seasonally flooded wetlands, *Geophys. Res. Lett.*, *34*, L15404, doi:10.1029/2007GL030156.

1. Introduction

[2]   Temporal and spatial changes in flood inundation extent and water heights are complex for large, remote floodplains such as those in the Amazon, yet are critical for understanding hydrological and biogeochemical processes in these important ecosystems. Despite several recent studies [*Coe et al.*, 2002; *Hamilton et al.*, 2002; *Alsdorf et al.*, 2005, 2007] the dynamics of seasonally flooded wetlands in the Amazon basin are not well quantified through ground or satellite observations or modeling. Yet Amazon river discharge comprises ~20% of total continental runoff [*Richey et al.*, 1989] and the dynamics of wetland inundation within the basin exert a strong control on processes such as plant productivity [*Wittman et al.*, 2004], heavy metal accumulation [*Silva et al.*, 2005], nutrient dynamics [*Melack and Forsberg*, 2001] and the carbon cycle [*Richey et al.*, 2002; *Melack et al.*, 2004].

[3]   Whilst the regional significance of Amazon wetland hydrology and biogeochemistry is undisputed, uncertainty remains because of an inability to measure or model non-linear inundation dynamics in remote basins at fine spatial and temporal resolutions. Of currently available data, ground observations of water surface elevation and discharge are spatially infrequent (up to 200 km apart on the central Amazon), river gauges are located only on main channels, and the Amazonian floodplain is entirely ungauged. Satellite observations of inundation extent and water level do not provide a solution as these can only be made using profiling altimeters with wide (100s of km) spacing between tracks [*Birkett et al.*, 2002], passive microwave instruments with good temporal but limited spatial resolution (0.25° pixels) [*Hamilton et al.*, 2002] or synthetic aperture radars with good spatial resolution (25 m pixels) but limited temporal coverage [*Hess et al.*, 2003]. Available models of Amazonian discharge are based on either: (a) Muskingum routing of main stem flow and a simple 'bathtub' floodplain representation where floodplain water levels are assumed equivalent to those in the main channel [*Richey et al.*, 1989] or (b) a coarse (~9 km) resolution 2D model [*Coe et al.*, 2002] that cannot resolve the spatial or temporal detail of floodplain hydraulic processes. The complexity of Amazonian floodplain flow at spatial scales of ~100 m and over periods of ~24 hours or more has recently been demonstrated by *Alsdorf et al.* [2005, 2007] and show previous models of Amazonian floodplain inundation to be of too coarse a resolution to capture floodplain inundation dynamics.

[4]   To improve estimates of the hydrological fluxes on seasonally flooded Amazonian wetlands we require a more detailed view of the dynamics of the inundation process. A solution to this is to use a 2D hydrodynamic model to simulate inundation over the Amazon floodplain, and sufficient flow, water level and inundation data now exist to drive and validate such a model. However, to date such codes have only been applied to small areas (model domains of no more than ~200 km²) due to computational cost. Moreover, such models have only been used to simulate short (<1 month long) events. Here we report the application of a recently developed and computationally efficient 2D hydrodynamic model to a ~13,000 km² section of the central Amazon floodplain in Brazil which allows, for the first time, this scale of application to be undertaken at sufficient resolution to resolve complex floodplain flow patterns. This paper represents the first reported application of a 2D hydrodynamic model at this scale, and the first validation of the ability of such a code (applied at any scale)

[1]Department of Geography, Tremough Campus, University of Exeter, Cornwall, UK.
[2]School of Geographical Sciences, University of Bristol, Bristol, UK.
[3]School of Earth Sciences, Ohio State University, Columbus, Ohio, USA.
[4]Setor de Ecología Laboratorio de Ecossistemas Aquáticos, Instituto Nacional de Pesquisas da Amazonas, Manaus, Brazil.
[5]Halcrow Group Ltd., Wiltshire, UK.
[6]Bren School of Environmental Science and Management, University of California, Santa Barbara, California, USA.
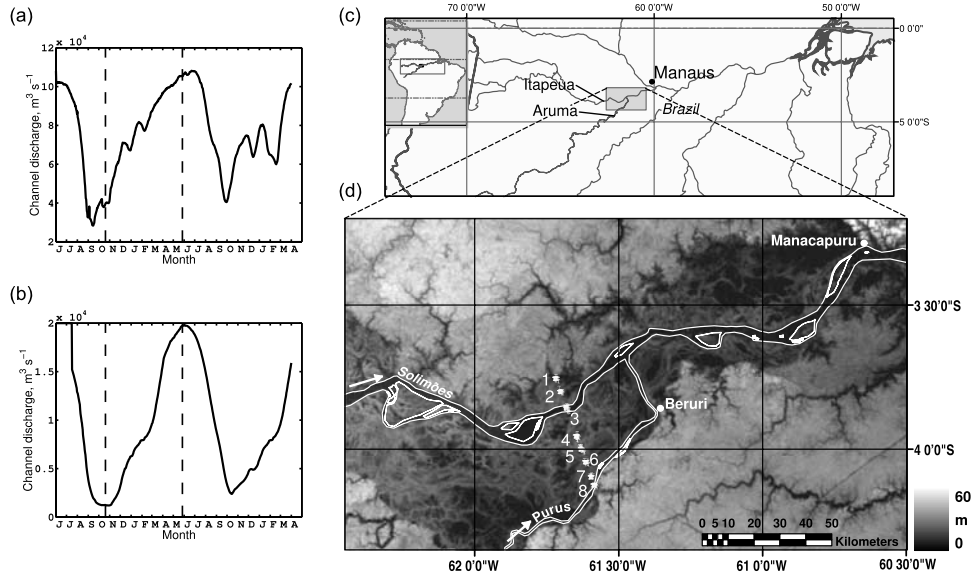[7]Department of Earth System Science, University of California, Irvine, California, USA.

Figure 1. Gauged flow data from 1 June 1995 to 31 March 1997 for (a) Solimões river (Itapeua) and (b) Purus river (Aruma): dashed lines indicate the timing of JERS-1 images; (c) overview map and (d) the study site showing the river channel and 270 m SRTM "bare earth" DEM, and the locations of available river stage data (Beruri and Manacapuru gauging stations) and satellite altimetry data (labeled 1–8) used for model validation.

to simulate full drainage of a topographically complex floodplain.

2. Modeling Approach

[5] 2D hydrodynamic models represent flooding dynamics by numerically solving equations for mass and momentum conservation. Boundary conditions are the time series of water fluxes into the modeled domain and are typically derived from gauging station information. Other critical input data are a 'bare earth' Digital Elevation Model (DEM) of sufficient resolution and vertical accuracy to capture floodplain topographic features relevant to flow development at the scale of interest and channel bathymetric information detailing the longitudinal slope.

[6] Full solutions of the shallow water equations may be computationally expensive and may not allow fine scale model application to large domains as required for simulation of Amazon floodplain inundation. Accordingly, we apply a simple coupled 1D/2D model, LISFLOOD-FP [Bates and De Roo, 2000] which aims to combine the best features of 1- and 2D models. Channel flow is represented using the kinematic approximation to the full 1D St. Venant equations solved using a fully implicit Newton-Raphson scheme. Floodplain flows are treated using a storage cell approach implemented for a raster grid to give an approximation to a 2D diffusive wave. Here we solve a continuity equation relating flow into a cell and its change in volume, and a momentum equation for each direction where flow between cells is calculated according to Manning's law:

$$Q^{i,j} = \frac{h_{\text{flow}}^{5/3}}{n}\left(\frac{h^{I-1,j} - h^{i,j}}{\Delta x}\right)^{1/2}\Delta x \qquad (1)$$

where $h^{i,j}$ is the water free surface height at the node (i, j), h_{flow} is the depth through which water can flow between two cells, Δx is the cell dimension, n is the Manning's friction coefficient, and Q describes the volumetric flow rate between floodplain cells. To prevent the build up of oscillations in areas of deep water with low free surface gradient, the flow limiter of Horritt and Bates [2001] was used. A complete description of the model is given by Bates and De Roo [2000]. The model simulates the time evolution of water depth in each model grid cell at each time step in response to main channel flood waves and represents the simplest physical representation capable of simulating dynamic floodplain inundation.

3. Model Application

[7] We applied LISFLOOD-FP to a ∼260 km reach of the Solimões River between Itapeua and Manaus, which includes the tributary with the Purus River and the associated 40 km wide confluence plain (see Figure 1). Terrain data were available from 90 m resolution DEM data from the Shuttle Radar Topography Mission (SRTM). SRTM data over South America have a mean absolute height accuracy of 1.7 m, with 90% of errors being less than 7.5 m [Rodriguez et al., 2006]. SRTM was flown in February 2000 during early rising water conditions along the Amazon main stem meaning that seasonally flooded wetlands and floodplains were predominantly dry and could be mapped. However, SRTM requires processing to remove vegetation artifacts in order to obtain a 'bare earth' DEM as the X and C band radars used do not fully penetrate vegetation canopies. To achieve this we conducted fieldwork in May 2005 along a 150 km reach of the Solimões River from Manaus upstream to the confluence with the Purus River to map vegetation heights in different habitats (flooded forest, woodlands and shrublands, grasslands). In total we sur-

veyed ∼10 km of vegetation heights and used this to develop representative canopy heights for each cover type. We also conducted ground and vegetation height surveys at the edge of deforested areas visible within recent Landsat 7 imagery and compared this to the SRTM transect across this vegetation boundary to estimate a canopy penetration depth for the radar signal of 50%, which is consistent with other studies conducted on SRTM data by NASA Jet Propulsion Laboratory (E. Rodriguez, personal communication, 2005). By combining these estimates with a vegetation cover type map developed by *Hess et al.* [2003] we were then able to remove vegetation artifacts from the SRTM data to create a first order 'bare earth' DEM for this reach.

[8] We aggregated the 90 m corrected SRTM data to 270 m (Figure 1d) and simulated a period between 1 June 1995 and 31 March 1997 using a hydrograph based on gauged data for the Itapeua and Aruma gauging stations on the Solimões and Purus rivers just upstream of the modeled domain. As noise in SRTM data is dominated by short correlation lengths (∼45–90 m scale), the pixel-to-pixel noise is uncorrelated and reduces linearly in proportion to $1/\sqrt{n}$ as the data are aggregated, where n is the number of pixels being averaged [*Rodriguez et al.*, 2006]. Thus for model grids at 270 m, 90% of the SRTM noise is <2.5 m. This is less than the amplitude of the Amazon flood pulse (∼10 m) and the vertical scale of the floodplain morphologic features (channels, levees, scroll bars of ∼3−5 m) that control the inundation process at this spatial scale. In addition, absolute height errors may need to be taken in account when comparing model predicted water surface elevations to those derived from gauge data or satellite radar altimetry.

[9] Channel topography was approximated using cross-sections at the upstream and downstream ends of the Solimões and Purus river reaches, at their confluence and at two intermediate points on the Solimões using data from a sonar survey that we conducted. These data were also used to obtain bankfull depth in the main channel, which may drive performance in channel/floodplain exchange. As a first order approximation we assumed that runoff and direct precipitation inputs to the floodplain balanced losses due to evapo-transpiration and infiltration. Detailed floodplain hydrologic processes were not considered. For these simulations we used two Manning friction parameters, one (n_{ch}) for each of the Solimões and Purus river channels and one (n_{fp}) for the floodplain.

[10] Simulations were run with a time step of 20 s for the full 22 month simulation period, together with an initial period of 10 months at high-water steady-state which allowed the floodplain to fill prior to the dynamic simulation phase that started with flood wave recession (an animation is provided as auxiliary material Animation S1[1], with n_{ch} = 0.028 (Solimões), n_{ch} = 0.031 (Purus) and n_{fp} = 0.1). This resulted in ∼4.2 million time steps for a grid of 900 × 460 cells. Each simulation took 14 days on a 3.0 GHz PC. In order to examine the model response to friction, we ran a matrix of 28 simulations with values of n_{ch} varying from 0.022 to 0.028 (Solimões) and 0.025 to 0.031 (Purus) in 0.001 increments and n_{fp} varying from 0.06 to 0.12 in 0.02

increments. Friction for the Solimões within the study reach was estimated at 0.025 ± 0.003 by *LeFavour and Alsdorf* [2005].

4. Model Testing

[11] Output from the model was compared to three independent validation data sets: (i) JERS-1 images of flood inundation extent at low (19 October 1995) and high water (26 May 1996); (ii) ground observations of water level from the Beruri and Manacapuru gauges internal to the model domain on the Purus and Solimões rivers; and (iii) floodplain water surface elevations derived from satellite altimetry data.

[12] To compare to model predicted inundation extent, the JERS-1 image mosaics were classified into three classes using the dual-season mapping method of *Hess et al.* [2003], aggregated into three classes: (i) flooded; (ii) nonflooded; and (iii) mixed. Accuracy for all simulations was then calculated using the measure of fit, F:

$$F = \frac{A_{obs} \cap A_{mod}}{A_{obs} \cup A_{mod}} \times 100 \qquad (2)$$

where A_{obs} and A_{mod} represent the sets of pixels observed to be inundated and predicted as inundated, respectively. F ranges between 0 (where observed and predicted areas are completely different) to 100 (where observed and predicted areas are identical). Using this equation and excluding the mixed class, fit at high water ranged from 57% with the lowest channel friction values (n_{ch}, Solimões: 0.022; n_{ch}, Purus: 0.025) to 73% with the highest (n_{ch}, Solimões: 0.028; n_{ch}, Purus: 0.031), with values of n_{fp} making little difference to accuracy. This is similar to the best prediction accuracies reported for previous inundation modeling studies with LISFLOOD-FP and other models [*Bates and De Roo*, 2000; *Horritt and Bates*, 2002]. At low water, accuracy was less (23%) with little difference made by friction values. A comparison between the model and JERS-1 inundation extents is shown in Figure 2 for this simulation. The model did well at high water with little over or under-prediction, but at low water the lack of full drainage of the floodplain caused over-prediction. At low water, areas of the floodplain become hydraulically disconnected from the river channels resulting in the ponds of water that then drain slowly back to the river through small channels (<10 m wide) or which dry out through evaporation and infiltration. These narrow connections between isolated compartments on the floodplain are unobserved by SRTM, and the aggregation to 270 m employed here further reduces our ability to resolve the complex, small scale topography that controls some of floodplain de-watering. Moreover, by not including floodplain hydrologic processes in our initial model we also reduce our ability to simulate low water inundation extent. Nevertheless, this study represents the first time that a hydrodynamic model (applied at any scale) has been employed to simulate full drainage of a topographically complex floodplain as such codes are typically developed to simulate high flows only over limited spatial extents. Our results can thus be used to inform the development of a new generation of hydrodynamic models designed for continuous simulation.
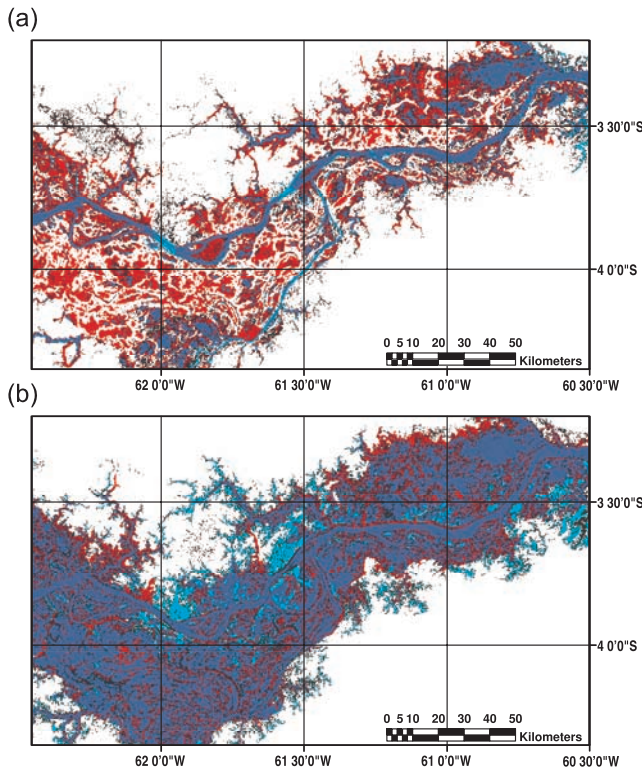
(a)

(b)

Figure 2. Comparison of model inundation extent with JERS-1 imagery at (a) low water and (b) high water: dark blue = areas inundated in both the JERS-1 image and the model prediction, red and cyan = over- and under-prediction by model, respectively, and black = uncertainty in the JERS-1 image.

[13] A comparison was also made between model output and water stage data (Figure 3) from the Beruri and Manacapuru gauging stations within the domain (see Figure 1d). The overall Root Mean Square Error (RMSE) for each was 3.56 m and 2.09 m, respectively, discounting the first 3 months where differences are due to the steady state conditions. Water levels matched closely for the Beruri gauge at high water and were under-predicted by ∼3 m at low water while, for Manacapuru, the model under-predicted stage by ∼2 m at high water and the first low water with the second low water predicted accurately. Whilst consideration of Froude and kinematic wave numbers shows the Amazon flood pulse to be a diffusion wave, Figure 3 indicates that the use of the kinematic wave in the channel and a diffusion wave on the floodplain as in the LISFLOOD-FP model provides a reasonable first order approximation.

[14] Comparison to satellite altimetry data for the full simulation at 8 locations across the floodplain (Figure 1d) is shown in Figure 4, with Figure 4i showing a scatter plot comparison for all data. The overall RMSE for all sites throughout the simulation was 2.37 m. This improved to 0.99 m during the high water period and worsened to 3.17 m during the low water periods. In most locations, the model predicts high water levels well (RMSE 0.17 to 1.83 m), whereas the accuracy of predictions at low water is less (RMSE 0.97 to 5.29 m). While low water estimates derived

from radar altimetry are associated with greatest uncertainty [*Birkett et al.*, 2002], the lack of dewatering in some locations of the floodplain is clear, particularly for sites 4 and 5 (Figures 4d and 4e) which are furthest from the main river channels. The primary cause of this seems to be problems with the terrain data, with, for example, the model grid elevation at site 4 (Figure 4d) being higher (∼22 m) than the low flow altimetry measurements of water surface elevation (∼18 m), making it impossible for the model to predict low water accurately. These errors are likely to be due to a combination of: (i) the coarse spatial sampling (90 m) and vertical error of the topographic data; (ii) the spatial aggregation of topography to 270 m; (iii) incomplete removal of vegetation artifacts from the raw SRTM data; and (iv) vertical and positional errors in the altimetry data. A secondary cause of the prevention of dewatering is the lack of infiltration in the floodplain. The net result of these errors are local disparities between model grid elevation values and water elevations measured by altimetry which may not be independent of the model grid scale.
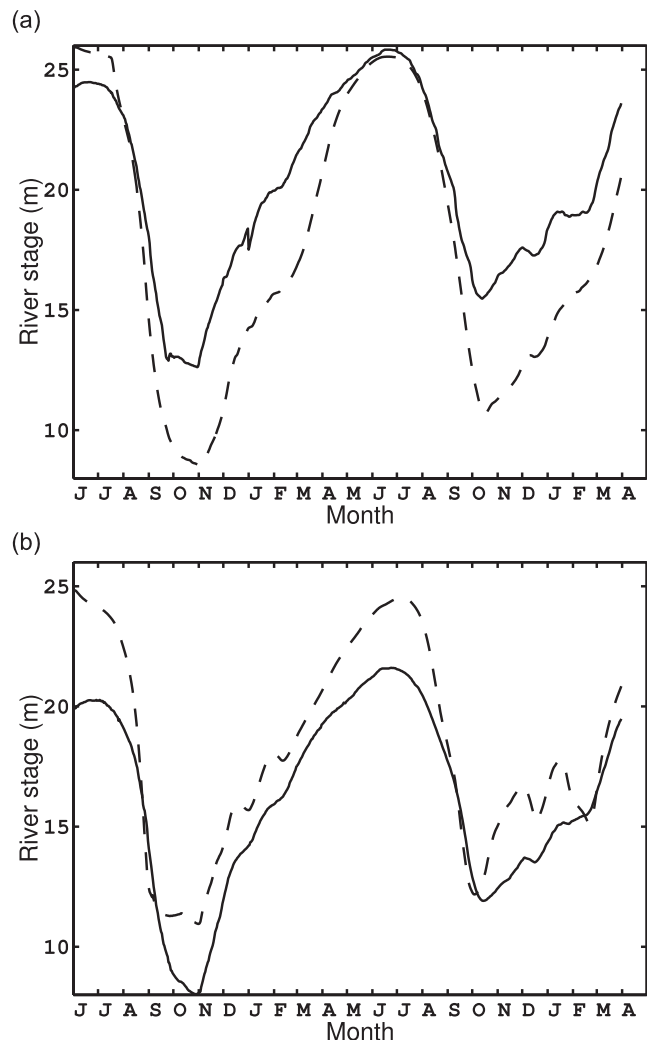
(a)

(b)

Figure 3. Gauged water level (solid line) compared to model water level (dashed line) for (a) Beruri (RMSE = 3.56 m) and (b) Manacapuru (RMSE = 2.09 m).
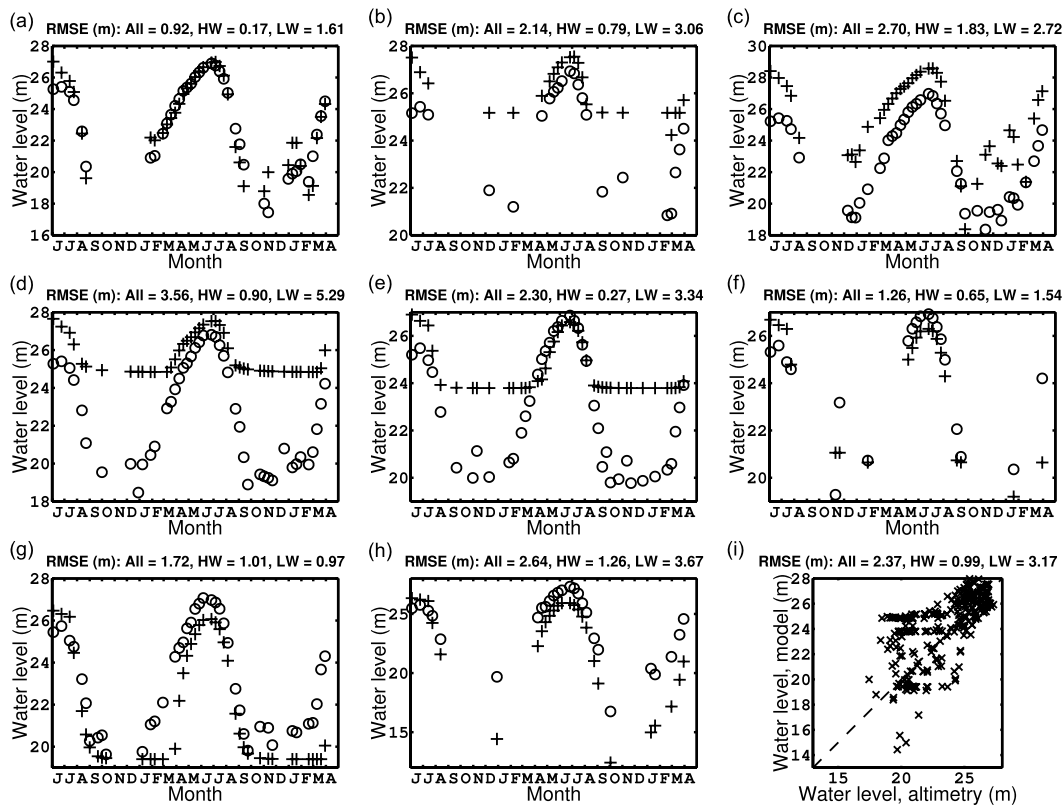
Figure 4. Altimetry water level (circles) compared to predicted water level (crosses) for locations (a–h) 1 through 8, respectively, with corresponding RMSE for the full simulation and at high water (HW: 1 May to 31 July) and low water (LW: 1 September to 30 November); (i) altimetry water level versus model water level for all available data and the overall RMSE.

[15]   Despite incomplete drainage of the floodplain at low water, the model provides a new and significantly more detailed view of floodplain hydraulics along this section of the Amazon that can enhance our understanding of flow pathways and residence times. For example, *Richey et al.* [1989] used Muskingum routing of main stem flow only and a simple 'bathtub' floodplain representation to estimate that approximately 30% of total Amazon flow volume is exchanged between the channel and floodplain at Itapeua. On the basis of more detailed 2D modeling and terrain data we estimate this exchange volume to be at least 40% between Itapeua and Manaus, and this is likely to be an underestimate due to over-prediction of inundation at low water. This has significant implications for our understanding of the chemical evolution of Amazon floodwaters and for the operation of biogeochemical cycles.

5. Conclusions

[16]   In this paper we show for the first time detailed, high-resolution floodplain water movements over a 22-month period for a large reach of the Amazon using JERS-1 images, gage observations, satellite altimetry data and a 1D/2D hydraulic model (LISFLOOD-FP). High-flow model simulations yield important new information on Amazon floodplain hydraulics, including an upward revision of the estimated volume of water exchanged between channel and floodplain. The wider implication of this research is that

predictions of floodplain inundation dynamics can now be used to as quantitative inputs to biochemical and geomorphic studies requiring detailed hydrodynamic information.

References

Alsdorf, D. E., T. Dunne, J. Melack, L. Smith, and L. Hess (2005), Diffusion modeling of recessional flow on central Amazonian floodplain, *Geophys. Res. Lett.*, *32*, L21405, doi:10.1029/2005GL024412.
Alsdorf, D. E., P. D. Bates, J. M. Melack, M. D. Wilson, and T. Dunne (2007), The spatial and temporal complexity of the Amazon flood measured from space, *Geophys. Res. Lett.*, *34*, L08402, doi:10.1029/2007GL029447.
Bates, P. D., and A. P. J. De Roo (2000), A simple raster-based model for floodplain inundation, *J. Hydrol.*, *236*, 54–77.
Birkett, C. M., L. A. K. Mertes, T. Dunne, M. H. Costa, and M. J. Jasinski (2002), Surface water dynamics in the Amazon Basin: Application of satellite radar altimetry, *J. Geophys. Res.*, *107*(D20), 8059, doi:10.1029/2001JD000609.
Coe, M. T., M. H. Costa, A. Botta, and C. Birkett (2002), Long-term simulations of discharge and floods in the Amazon Basin, *J. Geophys. Res.*, *107*(D20), 8044, doi:10.1029/2001JD000740.
Hamilton, S. E., S. J. Sippel, and J. M. Melack (2002), Comparison of inundation patterns among major South American floodplains, *J. Geophys. Res.*, *107*(D20), 8038, doi:10.1029/2000JD000306.
Hess, L. L., J. M. Melack, E. M. L. M. Novo, C. C. F. Barbosa, and M. Gastil (2003), Dual-season mapping of wetland inundation and vegetation for the central Amazon basin, *Remote Sens. Environ.*, *87*, 404–428.
Horritt, M. S., and P. D. Bates (2001), Predicting floodplain inundation: Raster-based modelling versus the finite element approach, *Hydrol. Processes*, *15*, 825–842.

Horritt, M. S., and P. D. Bates (2002), Evaluation of 1-D and 2-D numerical models for predicting river flood inundation, *J Hydrol.*, *268*, 87–99.

LeFavour, G., and D. Alsdorf (2005), Water slope and discharge in the Amazon River estimated using the shuttle radar topography mission digital elevation model, *Geophys. Res. Lett.*, *32*, L17404, doi:10.1029/2005GL023836.

Melack, J. M., and B. Forsberg (2001), Biogeochemistry of Amazon floodplain lakes and associated wetlands, in *The Biogeochemistry of the Amazon Basin and its Role in a Changing World*, edited by M. E. McClain, R. L. Victoria, and J. E. Richey, pp. 235-276, Oxford Univ. Press, New York.

Melack, J. M., L. L. Hess, M. Gastil, B. R. Forsberg, S. K. Hamilton, I. B. T. Lima, and E. M. L. M. Novo (2004), Regionalization of methane emissions in the Amazon Basin with microwave remote sensing, *Global Change Biol.*, *10*, 530–544.

Richey, J. E., L. A. K. Mertes, T. Dunne, R. L. Victoria, B. R. Forsberg, A. C. N. S. Tancredi, and E. Oliveira (1989), Source and routing of the Amazon River flood wave, *Global Biogeochem. Cycles*, *3*, 191–204.

Richey, J. E., J. M. Melack, A. K. Aufdenkampe, V. M. Ballester, and L. L. Hess (2002), Outgassing from Amazonian rivers and wetlands as a large tropical source of atmospheric CO_2, *Nature*, *416*, 617–620.

Rodriguez, E., C. S. Morris, and J. E. Belz (2006), A global assessment of the SRTM performance, *Photogramm. Eng. Remote Sens.*, *72*(3), 249–260.

Silva, D. S., M. Lucotte, M. Roulet, H. Poirier, D. Mergler, E. Santos, and M. Crossa (2005), Trophic structure and bioaccumulation of mercury in fish of three natural lakes of the Brazilian Amazon, *Water Air Soil Pollut.*, *165*, 77–94.

Wittman, F., W. J. Junk, and M. T. F. Piedade (2004), The varzea forests in Amazonia: Flooding and the highly dynamic geomorphology interact with natural forest succession, *For. Ecol. Manage.*, *196*, 199–212.

––––––––––––––––––

D. Alsdorf, School of Earth Sciences, Ohio State University, 275 Mendenhall Laboratory, 125 S. Oval Mall, Columbus, OH 43210, USA. (alsdorf@geology.ohio-state.edu)

P. Bates, School of Geographical Sciences, University of Bristol, Bristol BS8 1RJ, UK. (paul.bates@bristol.ac.uk)

J. Famiglietti and F. Frappart, Department of Earth System Science, University of California, Irvine, Croul Hall, Irvine, CA 92697-3100, USA. (jfamigli@uci.edu; ffrappar@uci.edu)

B. Forsberg, Setor de Ecología Laboratorio de Ecossistemas Aquâticos, Instituto Nacional de Pesquisas da Amazonas, Avenida Efigênio Sales 2239, Manaus, 69060-020, AM, Brazil. (forsberg@vivax.com.br)

M. Horritt, Halcrow Group Ltd., Burderop Park Swindon,Wiltshire SN4 0QD, UK. (horrittm@halcrow.com)

J. Melack, Bren School of Environmental Science and Management, University of California, Santa Barbara, Bren Hall, Room 2001, Santa Barbara, CA 93106-9610, USA. (melack@lifesci.ucsb.edu)

M. Wilson, Department of Geography, University of Exeter, Tremough Campus, Treliever Road, Penryn, Cornwall TR10 9EZ, UK. (matthew.d.wilson@ex.ac.uk)